Robotica (2016) volume 34, pp. 497–512. © Cambridge University Press 2014
doi:10.1017/S026357471400160X

Robust neural network control of MEMS gyroscope using adaptive sliding mode compensator

Juntao Fei†* and Yuzheng Yang‡

†*Jiangsu Key Laboratory of Power Transmission and Distribution Equipment Technology, Hohai University, Changzhou, China*
‡*College of IOT Engineering, Hohai University, Changzhou, China*

(Accepted June 2, 2014. First published online: July 4, 2014)

SUMMARY
A new robust neural sliding mode (RNSM) tracking control scheme using radial basis function (RBF) neural network (NN) is presented for MEMS z-axis gyroscope to achieve robustness and asymptotic tracking error convergence. An adaptive RBF NN controller is developed to approximate and compensate the large uncertain system dynamics, and a robust compensator is designed to eliminate the impact of NN modeling error and external disturbances for guaranteeing the asymptotic stability property. Moreover, another RBF NN is employed to learn the upper bound of NN modeling error and external disturbances, so the prior knowledge of the upper bound of system uncertainties is not required. All the adaptive laws in the RNSM control system are derived in the same Lyapunov framework, which can guarantee the stability of the closed loop system. Comparative numerical simulations for an MEMS gyroscope are investigated to verify the effectiveness of the proposed RNSM tracking control scheme.

KEYWORDS: MEMS gyroscope; Sliding mode control; Bound estimation; Neural network.

1. Introduction

An MEMS gyroscope is an angular velocity sensor which has been applied on many areas such as attitude control, consumer electronics, automobile, navigation, etc. However, fabrication imperfections and environmental variations result in a frequency mismatch and extra stiffness and damping couplings between two vibrating modes. Since 20 years ago, a lot of research has been investigated to control MEMS gyroscopes.

The adaptive controllers[1] drive both axes of vibration, and control the whole operation of the gyroscope. Leland[2] presented controllers to tune the drive axis oscillation to a fixed frequency and amplitude, and these drive the sense axis vibration to zero for force-to-rebalance operation. Salah *et al*.[3] developed a new control strategy to sense the time-varying angular rate for MEMS z-axis gyroscopes. Generally, the adaptive controllers presented earlier are based on the assumption that structure of the system model is known with unknown system parameters. However, not only system parameters but also the structure of the nonlinear system dynamics may be unknown for certain gyroscopes. It is difficult to design an appropriate adaptive control law for this kind of systems with conventional adaptive control algorithms. Fortunately, sliding mode control (SMC) is one of the most important approaches to deal with nonlinearities, uncertain dynamics, and bounded input disturbances with strong robustness. The main characteristic of the sliding mode control technique is its ability to provide strong robustness for control systems such that closed loop systems are completely insensitive to nonlinearities, uncertain dynamics, and bounded input disturbances in the sliding mode. In, ref. [4], Wang *et al*. developed the nonlinear dynamic model of a gyroscope system and used the SMC to guarantee the stability of the whole system. Fei *et al*.[5] incorporated the SMC strategy into adaptive control. Ebrahimi *et al*.[6] invoked a terminal SMC scheme to develop tracking control of the drive and sense modes. However, the problem using the previous control schemes

* Corresponding author. E-mail: jtfei@yahoo.com

is that all the upper and the lower bounds of unknown parameters need to be obtained before the commencement of the design of the controller and there is chattering in practical applications. The further research for the design of sliding mode controller without requirement of the prior knowledge of the uncertain bounds has been investigated by a number of researchers. For example, in refs. [7] and [8], an adaptive mechanism is developed to estimate the uncertain bound parameters and the estimates are then used as controller parameters to guarantee that effects of the system uncertainties can be eliminated and asymptotic error convergence can be obtained. Patompark *et al.*[9] proposed an adaptive backstepping SMC with bound estimation for underwater robotics vehicles. Since the neural network has the capability to approximate any nonlinear function over the compact input space, it can be utilized for interpolation and functional modeling. Neural network's learning ability to approximate arbitrary nonlinear functions makes it a useful tool for adaptive application. Lewis *et al.*[10] developed multilayer feed-forward neural network approaches for robot manipulator. Feng[11] presented a compensating scheme for robot tracking based on RBF NN. Lin *et al.*[12] used an NN-based robust nonlinear control for a magnetic levitation system. Man *et al.*[13] presented an adaptive back-propagation (BP) neural network controller. Adaptive neural sliding mode control for dynamic system and adaptive fuzzy sliding mode control for MEMS gyroscope have been investigated in refs. [21] and [22].

In this paper, a new robust neural network controller with sliding mode compensator using RBF networks is proposed for z-axis MEMS gyroscopes with uncertain dynamics and bounded input noises for achieving robustness and asymptotic tracking error convergence. An adaptive RBF NN controller is developed to approximate and compensate the large uncertain system dynamics, and a robust compensator is designed to eliminate the impact of NN approximating error and external disturbances, and guarantee the asymptotic stability property. Moreover, another RBF NN is employed to learn the upper bound of NN approximating error and external disturbances, so the prior knowledge of the upper bound of system uncertainties is relaxed. The control strategy proposed here has the following advantages compared to the existing ones:

1. The universal approximation property of RBF NN is adopted to approximate and cancel the unknown MEMS gyroscope dynamics. The deleterious impact of structured or unstructured uncertainties on tracking performance is weakened effectively. And no prior knowledge of the structure of the MEMS gyroscope is necessary.
2. The sliding mode compensator brings in strong robustness with respect to NN modeling error and external disturbances for the closed system. The tracking error is ensured to converge to zero asymptotically.
3. The deployment of the other RBF NN relaxes the requirement of the upper bound of the NN approximating error and external disturbances, which learns the upper bound of the uncertainties on-line. Compared to conservative, off-line estimation, the on-line fashion can eliminate the chattering phenomenon effectively and makes the control scheme easier for practical applications.

The paper is organized as follows. In Section 2, the dynamics of MEMS gyroscope is described and the problem is formulated. In Section 3, a robust neural network tracking control scheme for MEMS gyroscope is derived to guarantee the asymptotic stability of the closed loop system. In Section 4, an adaptive sliding mode compensator using RBF networks is designed to learn the upper bound of the uncertainties. Comparative simulation results are presented in Section 5 to demonstrate the effectiveness of the proposed robust NN controller with sliding mode compensator. Conclusions are given in Section 6.

2. MEMS Gyroscope Dynamics

Most MEMS gyroscopes are vibratory rate gyroscopes that have structures fabricated on polysilicon or crystal silicon, and the mechanical main component is a two degree-of-freedom vibrating structure, which is capable of oscillating on two orthotropic directions in a plane.[23] Vibratory gyroscopes behave like a mass attached to a rigid frame by springs, as shown in Fig. 1.

Vibratory gyroscopes provided an inertial measurement of rotation rate by sensing the effects of the Coriolis force in a rotating system. The mass is driven to vibrate along the drive axis. When the gyroscope is rotating about an axis perpendicular to the page, there will be a Coriolis force generated

https://doi.org/10.1017/S026357471400160X Published online by Cambridge University Press

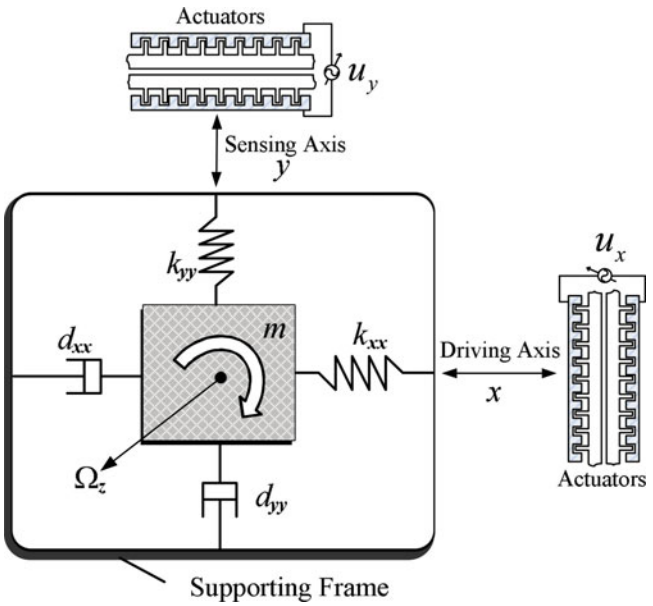

Fig. 1. Schematic diagram of a z-axis MEMS gyroscope.

along the sense axis, perpendicular to the drive and rotation axes. The Coriolis force causes the mass to move along the sense axis and the vibration is measured to determine the rotation rate.

To guarantee the stability and accuracy of the measurement of angular rate, the vibration of the proof mass must be stable, that is, keeping constant frequency and amplitude. To solve this issue, a trajectory following approach is used. Suppose that a reference trajectory is generated by an ideal oscillator and that the control objective is to make real trajectories of gyroscopes follow that of the reference model.

A typical MEMS gyroscope configuration includes a proof mass suspended by spring beams, electrostatic actuations, and sensing mechanisms for forcing an oscillatory motion and sensing the position and velocity of the proof mass, as well as a rigid frame which is rotated along the rotation axis. Dynamics of an MEMS gyroscope is derived from Newton's law in the rotating frame. For presentation simplicity, we will not describe the derivation procedure. For more details, please refer to ref. [24].

In a z-axis gyroscope, by supposing the stiffness of spring in the z-direction much larger than that in x, y directions, the motion of proof mass is constrained to only oscillate along the x–y plan. Assuming that the measured angular velocity is almost constant over a sufficiently long time interval, under typical assumptions $\Omega_x \approx \Omega_y \approx 0$, only the component of the angular rate Ω_z causes a dynamic coupling between the x- and y-axes. Taking fabrication imperfections into account, which cause extra coupling between x and y axes, the motion equation of a gyroscope is simplified as follows:

$$\begin{aligned} m\ddot{x} + d_{xx}\dot{x} + d_{xy}\dot{y} + k_{xx}x + k_{xy}y &= u_x + d_x + 2m\Omega_z\dot{y}, \\ m\ddot{y} + d_{xy}\dot{x} + d_{yy}\dot{y} + k_{xy}x + k_{yy}y &= u_y + d_y - 2m\Omega_z\dot{x}, \end{aligned} \tag{1}$$

where x and y are the coordinates of the proof mass with respect to the gyro frame in a Cartesian coordinate system; d_{xx}, d_{yy}, k_{xx}, k_{yy} are damping and spring coefficients; d_{xy}, k_{xy} called quadrature errors, are coupled damping and spring terms, respectively. They are mainly due to the asymmetries in suspension structure and misalignment of sensors and actuators; $u_{x,y}$ are the control forces, and $d_{x,y}$ denote the bounded input disturbances. The last two terms in (1), $2m\Omega_z\dot{y}$, $2m\Omega_z\dot{x}$, are the Coriolis forces and are used to reconstruct the unknown input angular rate Ω_z.

The following mild assumptions are used in this paper:

Assumption I: the mass of proof mass is constant, that is, $\dot{m} = 0$.

https://doi.org/10.1017/S026357471400160X Published online by Cambridge University Press

Assumption II: the coupled damping coefficient between x- and y-axes is much smaller than x-axis-self or y-axis-self ones, that is, $d_{xy} \ll d_{xx}, d_{xy} \ll d_{yy}$.

Rewriting the gyroscope dynamics (1) into vector form as

$$M\ddot{\boldsymbol{q}} + D\dot{\boldsymbol{q}} + K\boldsymbol{q} = \boldsymbol{\tau} - 2\Omega_z\dot{\boldsymbol{q}} + \boldsymbol{\tau}_d, \tag{2}$$

where

$$\boldsymbol{q} = \begin{bmatrix} x \\ y \end{bmatrix}, \boldsymbol{\tau} = \begin{bmatrix} u_x \\ u_y \end{bmatrix}, \boldsymbol{\tau}_d = \begin{bmatrix} d_x \\ d_y \end{bmatrix}, M = \begin{bmatrix} m & 0 \\ 0 & m \end{bmatrix},$$
$$D = \begin{bmatrix} d_{xx} & d_{xy} \\ d_{xy} & d_{yy} \end{bmatrix}, K = \begin{bmatrix} k_{xx} & k_{xy} \\ k_{xy} & k_{yy} \end{bmatrix}, \Omega = \begin{bmatrix} 0 & -m\Omega_z \\ m\Omega_z & 0 \end{bmatrix}.$$

All the MEMS gyroscope parameters in Eq. (2) cannot be known precisely. The model contains large uncertainties, slowly time-varying parameters, and even some nonlinearities.

Based on these previous assumptions, we have the following properties of the gyroscope system:

Property I: M is a constant symmetric positive-definite matrix.

Property II: The damping matrix D is a symmetric positive-definite matrix, and we suppose D is bounded.

Property III: The input disturbance is bounded by $\|\boldsymbol{\tau}_d\| \leq b_d$.

The control problem is to find a control law so that the proof mass position $\boldsymbol{q}(t)$ can track the desired trajectory $\boldsymbol{q}_d(t) = [x_d, y_d]^{\mathrm{T}}$. To achieve this control objective, define the tracking error $e(t) = \boldsymbol{q}_d(t) - \boldsymbol{q}(t)$. Meanwhile, define a sliding surface as

$$\boldsymbol{s}(t) = \dot{\boldsymbol{e}}(t) + \Lambda\boldsymbol{e}(t), \tag{3}$$

where $\Lambda = \Lambda^{\mathrm{T}} > 0$ is a design parameter matrix. Differentiating $\boldsymbol{s}$ and using Eq. (3), the MEMS gyroscope dynamics may be rewritten in terms of the sliding surface as

$$M\dot{\boldsymbol{s}} = -D\boldsymbol{s} - \boldsymbol{\tau} + \boldsymbol{f}(\boldsymbol{x}) - \boldsymbol{\tau}_d, \tag{4}$$

where $\boldsymbol{f}(\boldsymbol{x})$ denotes the unknown or uncertain gyroscope system dynamics

$$\boldsymbol{f}(\boldsymbol{x}) = M(\ddot{\boldsymbol{q}}_d + \Lambda\dot{\boldsymbol{e}}) + D(\dot{\boldsymbol{q}}_d + \Lambda\boldsymbol{e}) + K\boldsymbol{q} + 2\Omega\dot{\boldsymbol{q}} \tag{5}$$

and $\boldsymbol{x} \in \Re^{10}$ is the measurable signal vector

$$\boldsymbol{x} = \begin{bmatrix} \boldsymbol{e}^{\mathrm{T}} & \dot{\boldsymbol{e}}^{\mathrm{T}} & \boldsymbol{q}_d^T & \dot{\boldsymbol{q}}_d^T & \ddot{\boldsymbol{q}}_d^T \end{bmatrix}^{\mathrm{T}}. \tag{6}$$

To eliminate the effects of uncertain dynamics and external disturbances so that the output tracking error asymptotically converges to zero, a robust neural sliding mode tracking control system, which comprises an adaptive RBF NN controller and a variable structure compensator, is developed in the following section.

3. Robust Neural Network Control

Because of the great advantages of neural networks in dealing with approximation problems, an NN controller is developed in this section to approximate the unknown gyroscope system dynamics $\boldsymbol{f}(\boldsymbol{x})$ online and the output of the NN is used to compensate the impact of system uncertainties on tracking performance. A variable structure controller is designed to curb the NN modeling error and the bounded input disturbances for ensuring robustness and asymptotical tracking error convergence. The block diagram of the proposed RNSM control system is shown in Fig. 2. In our controller design, Eq. (4) is considered as the system model and the assumptions mentioned earlier are used.

https://doi.org/10.1017/S026357471400160X Published online by Cambridge University Press

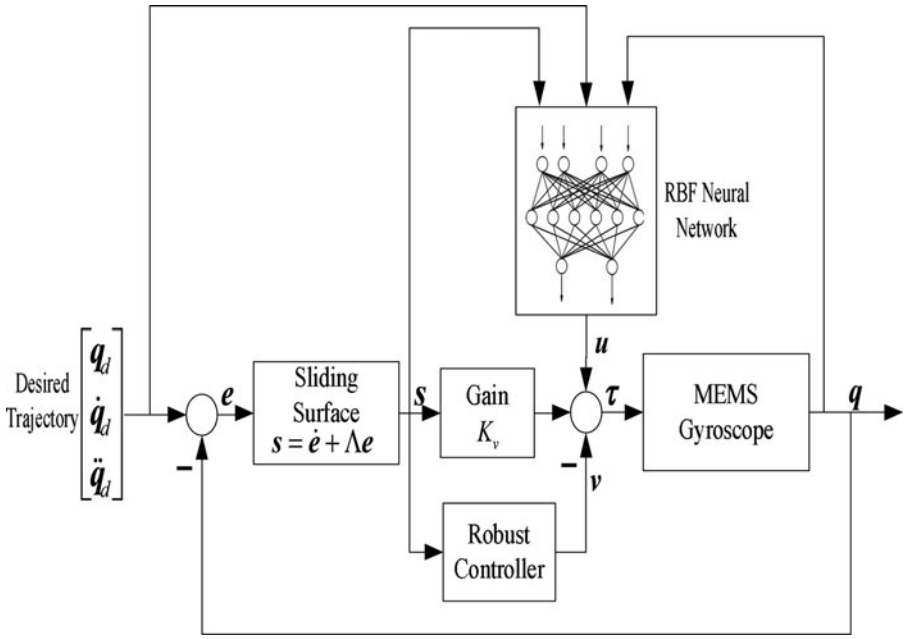

Fig. 2. Block diagram of RNSM control for MEMS gyroscope.

The following RBF NN is used to approximate system uncertainties $\boldsymbol{f}(\boldsymbol{x})$:

$$\boldsymbol{u} = \hat{\boldsymbol{f}}(\boldsymbol{x}) = \hat{W}^{\mathrm{T}}\boldsymbol{\phi}(\boldsymbol{x}), \tag{7}$$

where $\boldsymbol{x} \in \Re^{10}$ is the input of the RBF NN, defined in the last section; $\boldsymbol{u} \in \Re^2$ is the output of the NN; $W \in \Re^{n^* \times 2}$ is the NN weight matrix, in which n^* represents the hidden layer nodes; the vector $\boldsymbol{\phi}(\boldsymbol{x}) \in \Re^{n^*}$ is Gaussian type of active functions defined element-wise as

$$\phi_i(\boldsymbol{x}) = \exp\left(-\frac{\|\boldsymbol{x} - \boldsymbol{c}_i\|^2}{\sigma_i^2}\right), \quad i = 1, 2, \cdots, n^*. \tag{8}$$

Remark I: $c_i \in \Re^{10}$ and $\sigma_i \in \Re^1$, denoting the center and width of the ith hidden node, respectively, are predetermined and the local training technique in refs. [13] and 14] can be used to choose appropriate $\boldsymbol{c}_i$ and σ_i. Therefore, the adjustable NN weights $\hat{W}$ appear linearly with respect to the known nonlinear function $\boldsymbol{\phi}(\boldsymbol{x})$.

According to the universal approximation properties of the RBF NN[16], we may make the following assumption:

Assumption III: On a compact set S, there exists an optimal constant NN weight matrix W such that the output of the optimal RBF NN with enough hidden nodes satisfies:

$$\|\boldsymbol{\varepsilon}(\boldsymbol{x})\| = \left\|\boldsymbol{f}(\boldsymbol{x}) - W^{\mathrm{T}}\boldsymbol{\phi}(\boldsymbol{x})\right\| \leq \varepsilon_N, \tag{9}$$

where $\boldsymbol{\varepsilon}(\boldsymbol{x})$ is the reconstruction error due to the use of RBF NN and it is bounded by ε_N.

Remark II: The suitable optimal weight matrix may not be unique.[17] The "best" weights may then be defined as those which minimize the supremum norm over S of $\boldsymbol{\varepsilon}(\boldsymbol{x})$. The issue is not of major concern here, as we only need to know that such optimal weight exists; their actual values are not required. As to the modeling error $\boldsymbol{\varepsilon}(\boldsymbol{x})$, the more hidden nodes, the smaller value we shall expect, even zero.

Now, if the prior knowledge of the uncertain bound which includes the bound of the external disturbances and the NN modeling error is available, or it could be derived from some off-line

https://doi.org/10.1017/S026357471400160X Published online by Cambridge University Press

estimating methods,[17] we design the following robust compensator:

$$\boldsymbol{v} = (\varepsilon_N + b_d)\text{sgn}(\boldsymbol{s}), \tag{10}$$

where sgn() is a sign function and $\boldsymbol{v}$ is some switching control law.

The whole control law is taken as

$$\boldsymbol{\tau} = K_v \boldsymbol{s} + W^{\mathrm{T}}\boldsymbol{\phi}(\boldsymbol{x}) + (\varepsilon_N + b_d)\text{sgn}(\boldsymbol{s}) \tag{11}$$

where gain matrix $K_v = K_v^{\mathrm{T}} > 0$ and $K_v\boldsymbol{s} = K_v(\dot{\boldsymbol{e}} + \Lambda \boldsymbol{e})$ is a standard proportional-plus-derivative (PD) term.

Theorem I: Consider the MEMS gyroscope system dynamics represented by Eq. (4) with *Assumption I-III*, if the RNSM control law is designed as Eq. (11), in which the adaptive algorithm of the RBF NN weights is designed as

$$\dot{\hat{W}} = F\boldsymbol{\phi}(\boldsymbol{x})\boldsymbol{s}^{\mathrm{T}} \tag{12}$$

with arbitrary symmetric positive-definite matrix F, then the asymptotical stability of the closed system can be guaranteed and the output tracking error $\boldsymbol{e}(t)$ can asymptotically converge to zero.

Proof: Define the following Lyapunov function candidate for the RNSM control system

$$L = \frac{1}{2}\boldsymbol{s}^{\mathrm{T}} M \boldsymbol{s} + \frac{1}{2}\text{tr}\{\tilde{W}^{\mathrm{T}} F^{-1} \tilde{W}\}, \tag{13}$$

where tr() denotes the matrix trace operator, and $\tilde{W} = W - \hat{W}$.

Differentiating L with respect to time gives

$$\dot{L} = \boldsymbol{s}^{\mathrm{T}} M \dot{\boldsymbol{s}} + \text{tr}\{\tilde{W}^{\mathrm{T}} F^{-1} \dot{\tilde{W}}\}. \tag{14}$$

Substituting Eq. (4) and Eq. (11) into Eq. (14) yields

$$\dot{L} = -\boldsymbol{s}^{\mathrm{T}}(K_v + D)\boldsymbol{s} + \boldsymbol{s}^{\mathrm{T}}\tilde{W}^{T}\boldsymbol{\phi}(\boldsymbol{x}) + \boldsymbol{s}^{\mathrm{T}}(\boldsymbol{\varepsilon} - \boldsymbol{\tau}_d) - \boldsymbol{s}^{\mathrm{T}}(\varepsilon_N + b_d)\,\text{sgn}\,(\boldsymbol{s}) + \text{tr}\{\tilde{W}^{\mathrm{T}} F^{-1} \dot{\tilde{W}}\}. \tag{15}$$

Substituting the adaptive algorithm (12) into Eq. (15) and using the fact that $\dot{\tilde{W}} = -\dot{\hat{W}}$, we can obtain the following expression:

$$\dot{L} = -\boldsymbol{s}^{\mathrm{T}}(K_v + D)\boldsymbol{s} + \boldsymbol{s}^{\mathrm{T}}(\boldsymbol{\varepsilon} - \boldsymbol{\tau}_d) - \boldsymbol{s}^{\mathrm{T}}(\varepsilon_N + b_d)\text{sgn}(\boldsymbol{s}). \tag{16}$$

Next, we use some knowledge about vector norm

$$\begin{aligned} \boldsymbol{s}^{\mathrm{T}}(\boldsymbol{\varepsilon} - \boldsymbol{\tau}_d) - \boldsymbol{s}^{\mathrm{T}}(\varepsilon_N + b_d)\text{sgn}(\boldsymbol{s}) &\le \|s\| \cdot \|\boldsymbol{\varepsilon} - \boldsymbol{\tau}_d\| - (\varepsilon_N + b_d)\,\|s\| \\ &\le \|s\| \cdot (\|\boldsymbol{\varepsilon}\| + \|\boldsymbol{\tau}_d\|) - (\varepsilon_N + b_d)\,\|s\| \le 0. \end{aligned} \tag{17}$$

Using Eq. (17), Eq. (16) becomes:

$$\dot{L} \le -\boldsymbol{s}^{\mathrm{T}}(K_v + D)\boldsymbol{s} \le -\boldsymbol{s}^{\mathrm{T}} K_v \boldsymbol{s} \le -\lambda_{\min}(K_v)\,\|s\|^2 \le 0, \tag{18}$$

where $\lambda_{\min}(K_v)$ is the minimum eigenvalue of K_v and satisfies $\lambda_{\min} > 0$.

$\dot{L}$ is negative definite implies that $\boldsymbol{s}$ converges to zero. $\dot{L}$ is negative semidefinite ensures that L, $\boldsymbol{s}$, and $\tilde{W}$ are all bounded. It can be concluded from Eqs. (4) and (11) that $\dot{\boldsymbol{s}}$ is also bounded. The inequality (18) implies that $\boldsymbol{s}$ is integrable as $\int_0^t \|s\|^2 \mathrm{d}t \le \frac{1}{\lambda_{\min}}[L(0) - L(t)]$. Since $L(0)$ is bounded and $L(t)$ is nonincreasing and bounded, it can be concluded that $\lim_{t\to\infty}\int_0^t \|\boldsymbol{s}\|^2 \mathrm{d}t$ is bounded. Since $\lim_{t\to\infty}\int_0^t \|\boldsymbol{s}\|^2 \mathrm{d}t$, $\boldsymbol{s}$ and $\dot{\boldsymbol{s}}$ are all bounded, according to Barbalat's lemma,[19] $\lim_{t\to\infty} \boldsymbol{s}(t) = 0$,

https://doi.org/10.1017/S026357471400160X Published online by Cambridge University Press

that is $\boldsymbol{s}(t)$ will asymptotically converge to zero. As seen from Eq. (3), $\boldsymbol{e}(t)$ also converges to zero asymptotically.

Remark III: It can be seen from *Theorem I* that the prior knowledge of the upper bound of the uncertainties is required in the robust compensator design (10). Although there are some methods for off-line estimating the bound parameters in expression (10), the estimates of the uncertain bound parameters are very conservative, and the control input signals using the conservative estimates as the controller parameter are then very large. Therefore, implementation of the robust control scheme presented earlier in a practical situation might generate serious chattering phenomenon.

4. Adaptive Sliding Compensator Using RBF NN

To relax the requirement of the upper bound of system uncertainties in the design of a robust compensator (10), an adaptive sliding mode control scheme is investigated in this section, in which another RBF NN is adopted to adjust the sliding mode gain in a switching control law on-line to satisfy the sliding mode condition and guarantee the convergence of tracking error.

Let $\boldsymbol{\rho}$ represent the lumped RBF NN reconstruction error and external disturbances

$$\boldsymbol{\rho}(t) = \boldsymbol{\varepsilon}(t) - \boldsymbol{\tau}_d(t). \tag{19}$$

Due to the bound of $\boldsymbol{\varepsilon}(t)$ and $\boldsymbol{\tau}_d(t)$, we suppose $\boldsymbol{\rho}(t)$ is bounded by $\|\boldsymbol{\rho}(t)\| < \bar{\rho}(t)$. If the upper bound value $\bar{\rho}(t)$ cannot be measured, the following RBF NN is used to adaptively lean the upper bound of $\boldsymbol{\rho}$:

$$\hat{\bar{\rho}}(x, \boldsymbol{\theta}) = \hat{\boldsymbol{\theta}}^{\mathrm{T}} \phi_2(x), \tag{20}$$

where x is the input of the RBF NN, as described in the second section; $\boldsymbol{\theta} \in \Re^m$ is the weight vector of the RBF NN, and m is the number of hidden nodes. Vector $\phi_2(\boldsymbol{x}) \in \Re^m$ is also a Gaussian type of function. As seen from Eqs. (7) and (20), the two RBF neural networks have the similar structure, but their hidden nodes may be different and they play different roles in the control system.

For further analysis, we make the following assumptions:

Assumption IV: Given an arbitrary small positive constant ε^* and a continuous function $\bar{\rho}(t)$ on a compact set U, there exists an optimal weight vector $\boldsymbol{\theta}$ such that the output of the optimal neural network with enough nodes satisfies

$$|\varepsilon_2(\boldsymbol{x})| = \left|\boldsymbol{\theta}^{\mathrm{T}} \boldsymbol{\phi}_2(\boldsymbol{x}) - \bar{\rho}(t)\right| < \varepsilon^*. \tag{21}$$

Assumption V: The norm of the system uncertainties and its upper bound satisfy the following inequality on the compact set U:

$$\bar{\rho}(t) - \|\boldsymbol{\rho}(t)\| > \varepsilon_0 > \varepsilon^*. \tag{22}$$

Using the second RBF NN, we modify the control law as

$$\boldsymbol{\tau} = K_v \boldsymbol{s} + W^{\mathrm{T}} \boldsymbol{\phi}(x) + \hat{\boldsymbol{\theta}}^{\mathrm{T}} \boldsymbol{\phi}_2(x) \mathrm{sgn}(\boldsymbol{s}). \tag{23}$$

This new control law gives the following closed loop equation:

$$M\dot{\boldsymbol{s}} = -(K_v + D)\boldsymbol{s} + \tilde{W}^{\mathrm{T}} \boldsymbol{\phi}(x) + (\boldsymbol{\varepsilon} - \boldsymbol{\tau}_d) - \hat{\boldsymbol{\theta}}^{\mathrm{T}} \boldsymbol{\phi}_2(x) \mathrm{sgn}(\boldsymbol{s}). \tag{24}$$

Here, we propose two RBF neural networks. One of them is used to approximate and compensate the unknown MEMS gyroscope dynamics and it is described in the last section. The other is adopted

https://doi.org/10.1017/S026357471400160X Published online by Cambridge University Press

to learn the upper bound of NN modeling error and external disturbances. And we have the following theorem:

Theorem II: Consider the MEMS gyroscope represented by Eq. (4) with *Assumption I–II*. Let the control input for (4) be given by (23), in which *Assumptions III*, *IV,* and *V* about the two RBF NNs are satisfied. If the weight adaptive laws of the two RBF NNs are designed as Eqs. (12) and (25), respectively, then the output tracking error $\boldsymbol{e}(t)$ can asymptotically converge to zero

$$\dot{\hat{\boldsymbol{\theta}}} = \eta \cdot \|\boldsymbol{s}\| \cdot \boldsymbol{\phi}_2(x), \tag{25}$$

where η is a arbitrary positive value.

Proof: Define the following Lyapunov function candidate for the closed loop system (24):

$$L = \frac{1}{2}\boldsymbol{s}^{\mathrm{T}} M \boldsymbol{s} + \frac{1}{2}\mathrm{tr}\{\tilde{W}^{\mathrm{T}} F^{-1} \tilde{W}\} + \frac{1}{2}\eta^{-1}\tilde{\theta}^{\mathrm{T}}\tilde{\theta}, \tag{26}$$

where $\tilde{\boldsymbol{\theta}} = \boldsymbol{\theta} - \hat{\boldsymbol{\theta}}$.

Differentiate L with respect to time along the trajectory defined by Eq. (24)

$$\begin{aligned}\dot{L} &= \boldsymbol{s}^{\mathrm{T}} M \dot{\boldsymbol{s}} + \mathrm{tr}\{\tilde{W}^{\mathrm{T}} F^{-1} \dot{\tilde{W}}\} + \eta^{-1}\tilde{\theta}^{\mathrm{T}}\dot{\tilde{\boldsymbol{\theta}}} \\ &= -\boldsymbol{s}^{\mathrm{T}}(K_v + D)\boldsymbol{s} + \boldsymbol{s}^{\mathrm{T}}\tilde{W}^{\mathrm{T}}\boldsymbol{\phi}(\boldsymbol{x}) + \boldsymbol{s}^{\mathrm{T}}\boldsymbol{\rho} - \boldsymbol{s}^{\mathrm{T}}\hat{\theta}^{\mathrm{T}}\boldsymbol{\phi}_2(\boldsymbol{x})\,\mathrm{sgn}\,(\boldsymbol{s}) + \mathrm{tr}\{\tilde{W}^{\mathrm{T}} F^{-1}\dot{\tilde{W}}\} - \eta^{-1}\tilde{\theta}^{\mathrm{T}}\dot{\hat{\boldsymbol{\theta}}}.\end{aligned} \tag{27}$$

Substituting adaptive law (12) into Eq. (27), one can get

$$\begin{aligned}\dot{L} &= -\boldsymbol{s}^{\mathrm{T}}(K_v + D)\boldsymbol{s} + \boldsymbol{s}^{\mathrm{T}}\boldsymbol{\rho} - \boldsymbol{s}^{\mathrm{T}}\hat{\theta}^{\mathrm{T}}\boldsymbol{\phi}_2(\boldsymbol{x})\mathrm{sgn}(s) - \eta^{-1}\tilde{\theta}^{\mathrm{T}}\dot{\hat{\boldsymbol{\theta}}} \\ &= -s^{\mathrm{T}}(K_v + D)\boldsymbol{s} + \boldsymbol{s}^{\mathrm{T}}\boldsymbol{\rho} - \|\boldsymbol{s}\|\left[\hat{\theta}^{\mathrm{T}}\phi_2(\boldsymbol{x}) - \bar{\rho}(t) + \bar{\rho}(t)\right] - \eta^{-1}\tilde{\theta}^{\mathrm{T}}\dot{\hat{\boldsymbol{\theta}}} \\ &\le -\boldsymbol{s}^{\mathrm{T}}(K_v + D)\boldsymbol{s} - \|\boldsymbol{s}\|\left[\hat{\theta}^{\mathrm{T}}\phi_2(\boldsymbol{x}) - \bar{\rho}(t)\right] - \|\boldsymbol{s}\|\left[\bar{\rho}(t) - \|\boldsymbol{\rho}\|\right] - \eta^{-1}\tilde{\theta}^{\mathrm{T}}\dot{\hat{\boldsymbol{\theta}}}.\end{aligned} \tag{28}$$

Substituting adaptive law (25) into Eq. (28) yields

$$\begin{aligned}\dot{L} &\le -\boldsymbol{s}^{\mathrm{T}}(K_v + D)\boldsymbol{s} - \|\boldsymbol{s}\|\left[\hat{\theta}^{\mathrm{T}}\phi_2(\boldsymbol{x}) - \theta^{\mathrm{T}}\phi_2(\boldsymbol{x}) + \varepsilon_2(\boldsymbol{x})\right] - \|\boldsymbol{s}\|\left[\bar{\rho}(t) - \|\boldsymbol{\rho}\|\right] - (\boldsymbol{\theta}^{\mathrm{T}} - \hat{\theta}^{\mathrm{T}})\,\|\boldsymbol{s}\|\,\phi_2(\boldsymbol{x}) \\ &= -\boldsymbol{s}^{\mathrm{T}}(K_v + D)\boldsymbol{s} - \|\boldsymbol{s}\|\,\varepsilon_2(\boldsymbol{x}) - \|\boldsymbol{s}\|\left[\bar{\rho}(t) - \|\boldsymbol{\rho}\|\right] \\ &\le -\boldsymbol{s}^{\mathrm{T}}(K_v + D)\boldsymbol{s} + \|\boldsymbol{s}\|\,|\boldsymbol{\varepsilon}_2(\boldsymbol{x})| - \|\boldsymbol{s}\|\left[\bar{\rho}(t) - \|\boldsymbol{\rho}\|\right] \\ &= -\boldsymbol{s}^{\mathrm{T}}(K_v + D)\boldsymbol{s} + \|\boldsymbol{s}\|\left[|\varepsilon_2(\boldsymbol{x})| - (\bar{\rho}(t) - \|\boldsymbol{\rho}\|)\right] \le -\boldsymbol{s}^{\mathrm{T}}(K_v + D)\boldsymbol{s} + \|\boldsymbol{s}\|\,(\varepsilon^* - \varepsilon_0) \\ &< -\boldsymbol{s}^{\mathrm{T}}(K_v + D)\boldsymbol{s} \le -\boldsymbol{s}^{\mathrm{T}}K_v\boldsymbol{s} \le \boldsymbol{0}.\end{aligned} \tag{29}$$

From Eq. (29), we can conclude

$$\dot{L} < 0. \tag{30}$$

Equation (30) is the reaching condition for the sliding variable vector $\boldsymbol{s}$ to reach the sliding mode in a finite time

$$\boldsymbol{s} = \dot{\boldsymbol{e}} + \Lambda\boldsymbol{e} = 0. \tag{31}$$

On the sliding mode, error dynamics of the closed loop system has the following form:

$$\dot{\boldsymbol{e}} = -\Lambda\boldsymbol{e}. \tag{32}$$

Therefore, the proposed control system is asymptotically stable, and the tracking error $\boldsymbol{e}(t)$ asymptotically converges to zero.

https://doi.org/10.1017/S026357471400160X Published online by Cambridge University Press

Table I. Parameters of the gyroscope.

Parameter	Value
m	1.8×10^{-7}kg
k_{xx}	$63.955\text{N}/\text{m}$
k_{yy}	$95.92\text{N}/\text{m}$
k_{xy}	$12.779\text{N}/\text{m}$
d_{xx}	$1.8 \times 10^{-6}\text{N} \cdot \text{s}/\text{m}$
d_{yy}	$1.8 \times 10^{-6}\text{N} \cdot \text{s}/\text{m}$
d_{xy}	$3.6 \times 10^{-7}\text{N} \cdot \text{s}/\text{m}$

Remark IV: Unlike the fixed gain compensator designed in the last section, the prior knowledge of the upper bound of the NN modeling error and external disturbances is not required here. Instead, another adaptive RBF NN is introduced to estimate the upper bound of system uncertainties on-line and its output is used as compensator parameter to guarantee that impacts of the NN modeling error and external disturbances can be eliminated. Asymptotic error convergence can be obtained. Compared with the off-line, conservative and large estimates of the upper bound, the proposed adaptive sliding mode compensator using RBF NN can restrain the chattering phenomenon of control force effectively. So, it will be easily implemented for practical application. For any MEMS gyroscope, only a Gaussian network is needed to learn the upper bound of system uncertainties adaptively, which can guarantee the good tracking performance and strong robustness.

Remark V: It can be seen from the previous theorems that the weights of the two RBF NNs are updated based on Lyapunov stability theory. However, the guaranteed convergence of tracking error does not simply imply convergence of the weight estimates to their optimal values. The persistent excitation condition[20] should be satisfied for the estimates to converge to their optimal values. But it is not the concern for our tracking control purpose.

5. Simulation Analysis

A simulation example with a z-axis vibratory MEMS gyroscope is utilized in this section for the purpose of evaluating the performance of the proposed control scheme. The parameters of the MEMS gyroscope[1] are given in Table I.

The unknown angular velocity is assumed to be $\Omega_z = 100\ \text{rad}/\text{s}$. The desired trajectory is defined as

$$\boldsymbol{q}_d = [0.1\cos(\omega_1 t), 0.1\cos(\omega_2 t)]^{\mathrm{T}} \mu\text{m}. \tag{33}$$

where $\omega_1 = 6.17\ \text{rad}/\text{s}$, $\omega_2 = 5.11\text{rad}/\text{s}$. Unless specified, all the units for displacements are micron (μm), and micro-Newton (μN) for forces, which include control inputs, unknown dynamics, and their estimates, and external disturbances. We consider the following external disturbances:

$$\boldsymbol{\tau}_d = [(\sin(6.17t))^2 + \cos(5.11t), \quad (\sin(5.11t))^2 + \cos(6.17t)]^{\mathrm{T}} \mu\text{N}. \tag{34}$$

In our numerical simulations, we took the PD term gain matrix as $K_v = 100I$ with I representing the identity matrix. The tracking response under the sole PD controller with MEMS gyroscope being zero initial condition is shown in Figs. 3 and 4.

It can be seen obviously from Figs. 3 and 4 that the tracking performance is not acceptable under the sole PD controller, though the whole system is still stable. The unknown MEMS gyroscope dynamics $f(x)$ and external disturbances $\boldsymbol{\tau}_d$ degrade the tracking performance and their deleterious effect should be canceled by our proposed RNSM control scheme. An adaptive RBF NN is used to approximate the unknown dynamics $f(x)$ and a fixed-gain robust compensator is adopted to eliminate the impact of NN modeling error and external disturbances.

It can also be observed from Figs. 3 and 4 that the tracking error $\boldsymbol{e}(t)$ belongs to a compact in the error vector space $\boldsymbol{e}$ with center at origin and each side length about 0.05. We will constrain our attention on that compact set when designing the RBF NN approximator. We selected 45 hidden

https://doi.org/10.1017/S026357471400160X Published online by Cambridge University Press

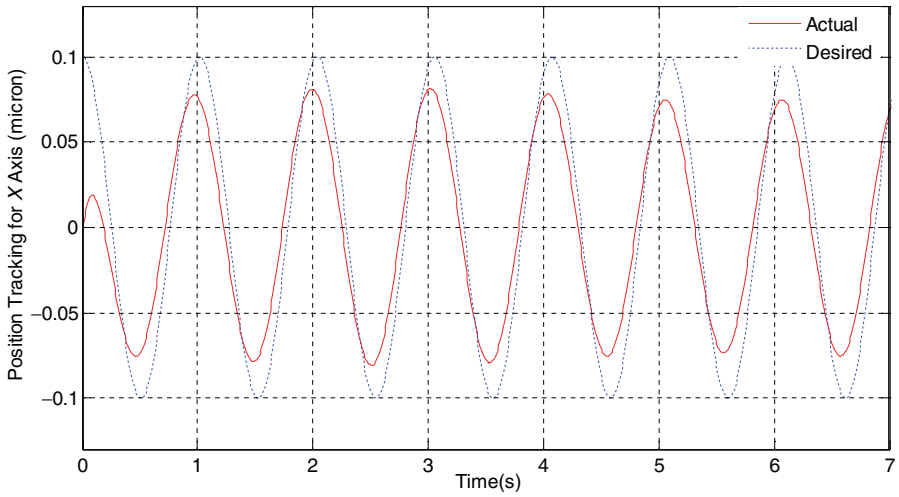

Fig. 3. Position tracking for *x*-axis under the sole PD controller.

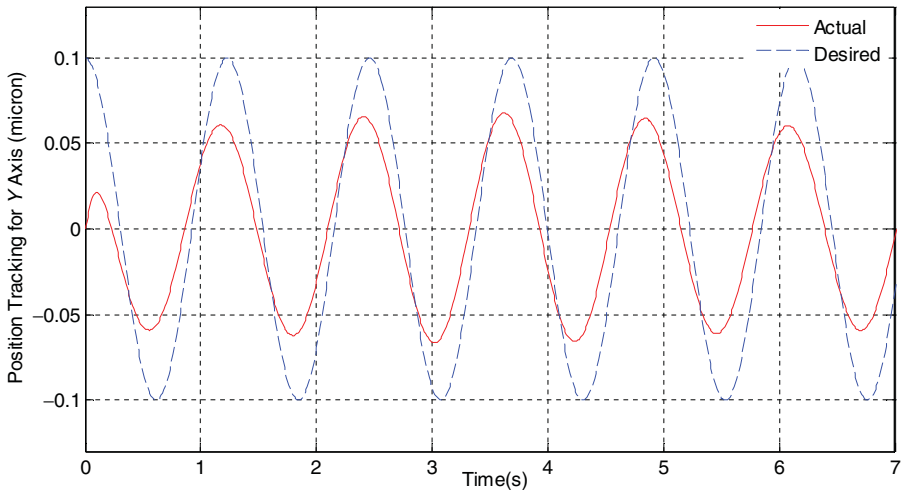

Fig. 4. Position tracking for *y*-axis under the sole PD controller.

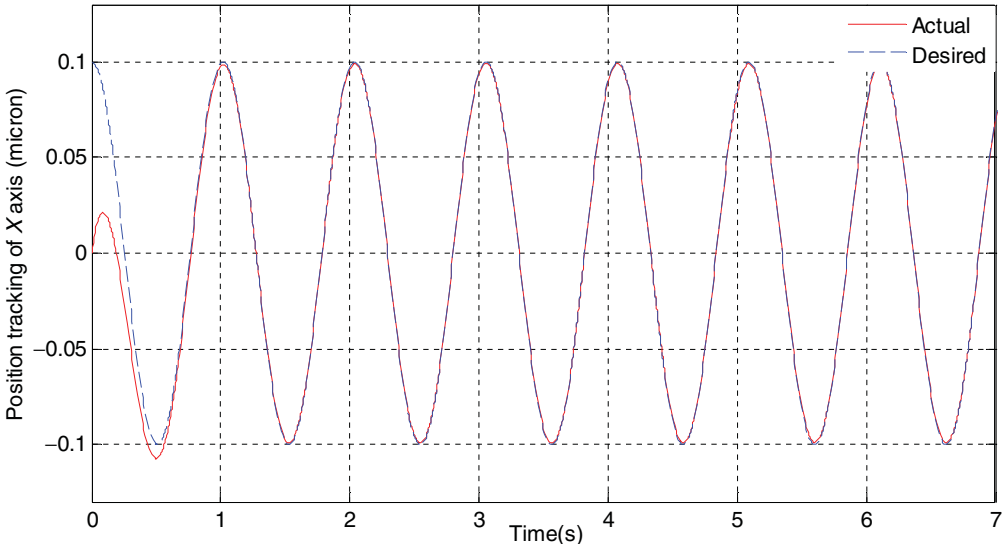

Fig. 5. Position tracking for *x*-axis under the RNSM controller.

https://doi.org/10.1017/S026357471400160X Published online by Cambridge University Press

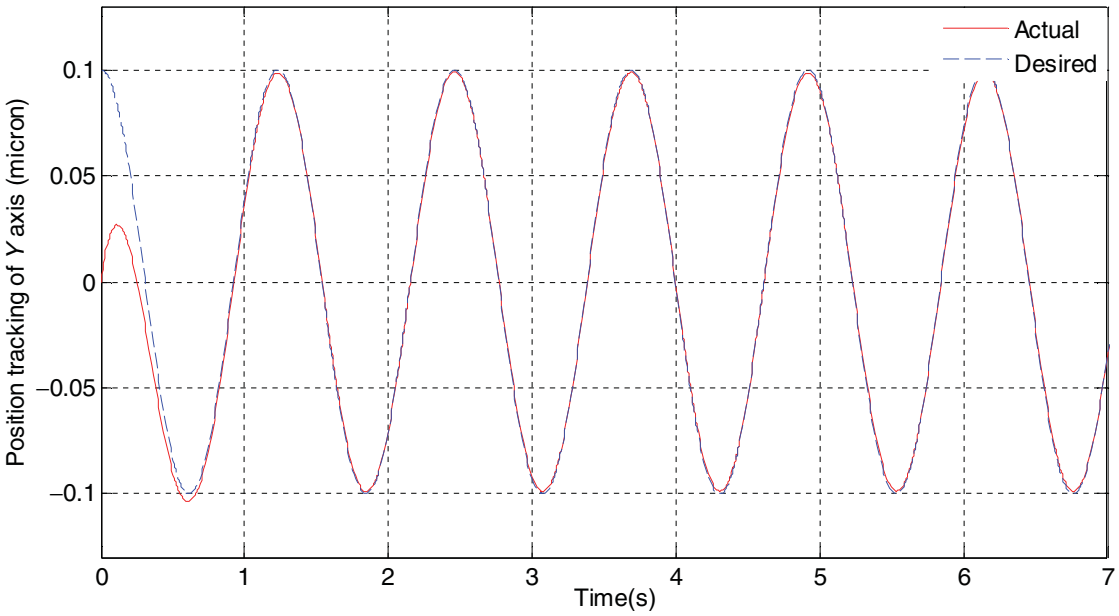

Fig. 6. Position tracking for y-axis under the RNSM controller.

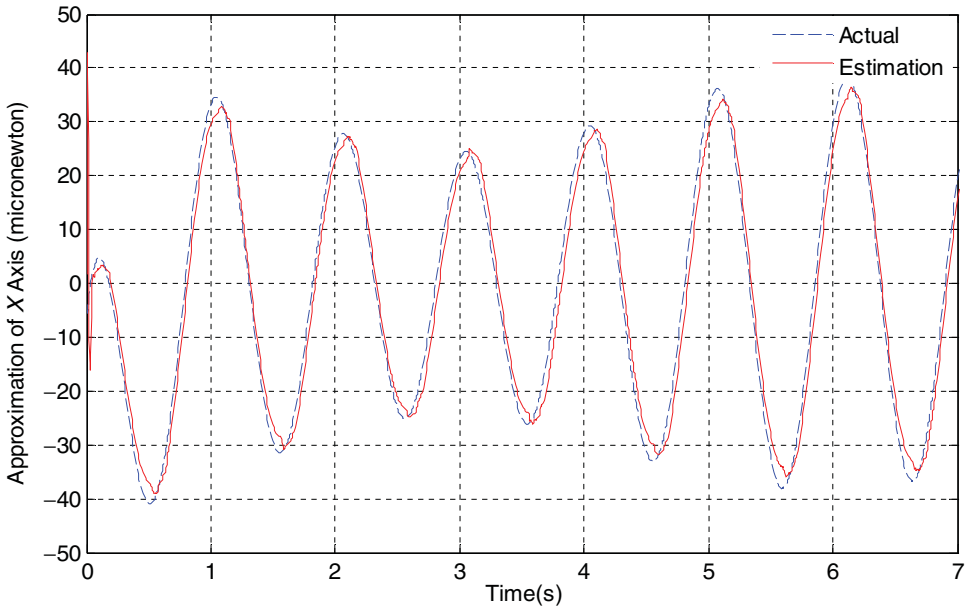

Fig. 7. NN approximation for x-axis component of $f(x)$.

layer nodes and took width $\sigma = 2$. The adaptive law gain was chosen as $F = \text{diag}\{500, 500\}$; Sliding surface parameter $\Lambda = \text{diag}\{5, 5\}$; $K_v = 100I$ remained unchanged. We took $\varepsilon_N = 1$ and $b_d = 2$ for the design of fixed-gain robust compensator.

Figs. 5, 6, 7, and 8 show the simulation results under the proposed RNSM controller. Zero initial condition is chosen for the states of the MEMS gyroscope. Figs. 5 and 6 demonstrate the good tracking performance of the proof mass trajectories along x-axis and y-axis, respectively. Figs. 7 and 8 show the impressive approximation of RBF NN to unknown dynamics $f(x)$. As shown in the two figures, RBF NN is able to approximate the unknown gyroscope dynamics quickly using the measurable signals x throughout the whole compact set. Though there exists NN modeling error, the tracking error asymptotically converges to zero.

https://doi.org/10.1017/S026357471400160X Published online by Cambridge University Press

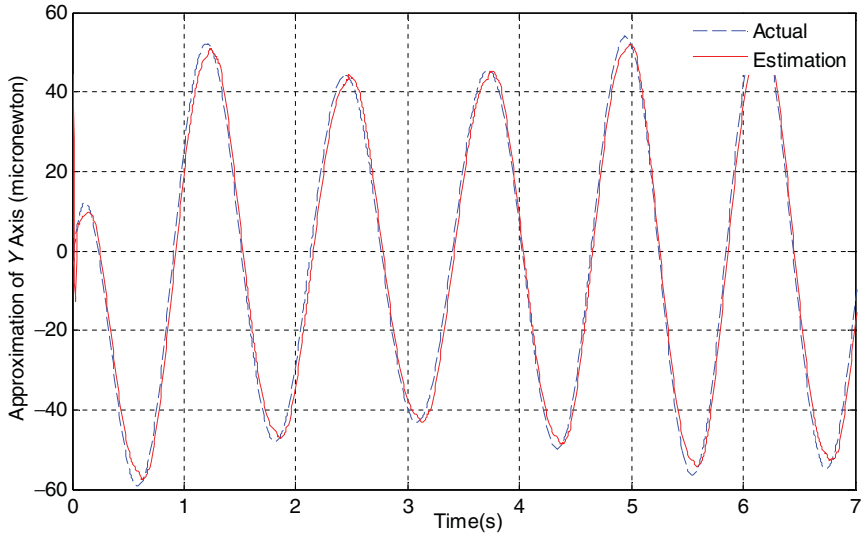

Fig. 8. NN approximation for y-axis component of $f(x)$.

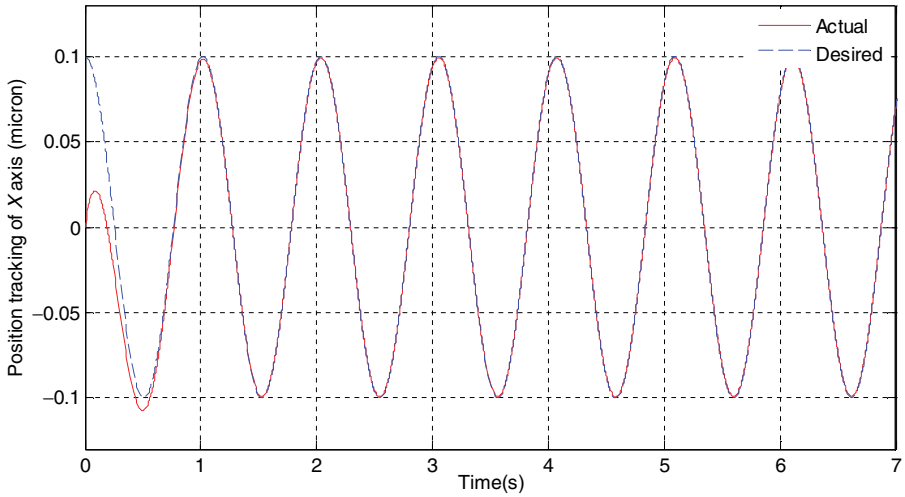

Fig. 9. Position tracking for x-axis under ASMC.

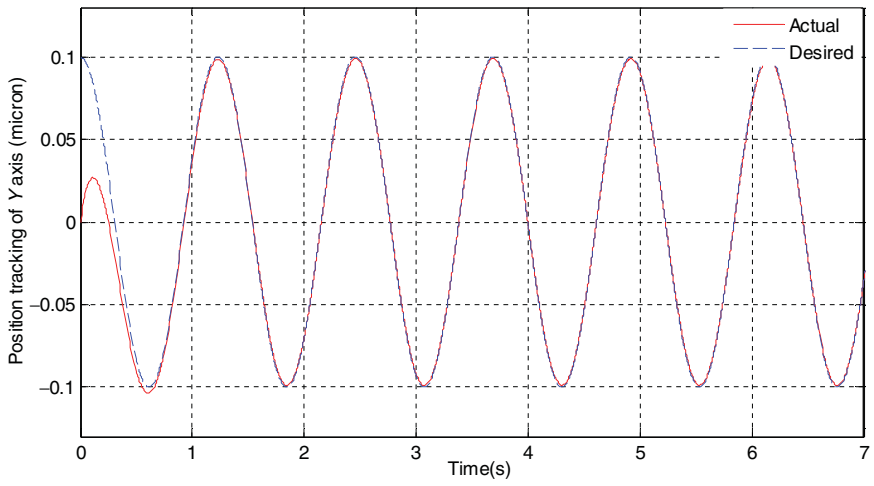

Fig. 10. Position tracking for y-axis under ASMC.

https://doi.org/10.1017/S026357471400160X Published online by Cambridge University Press

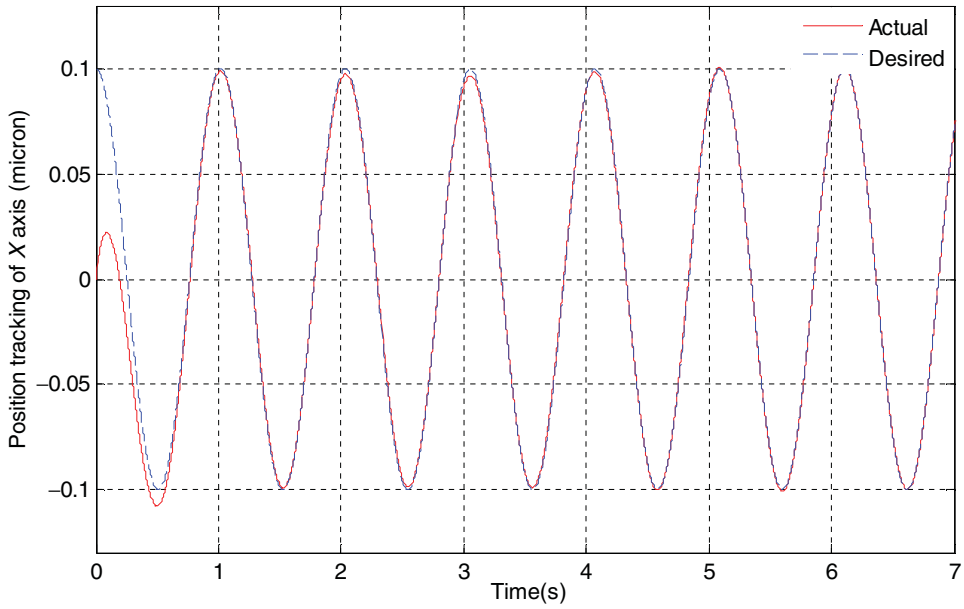

Fig. 11. Position tracking for x-axis under the RNSM controller.

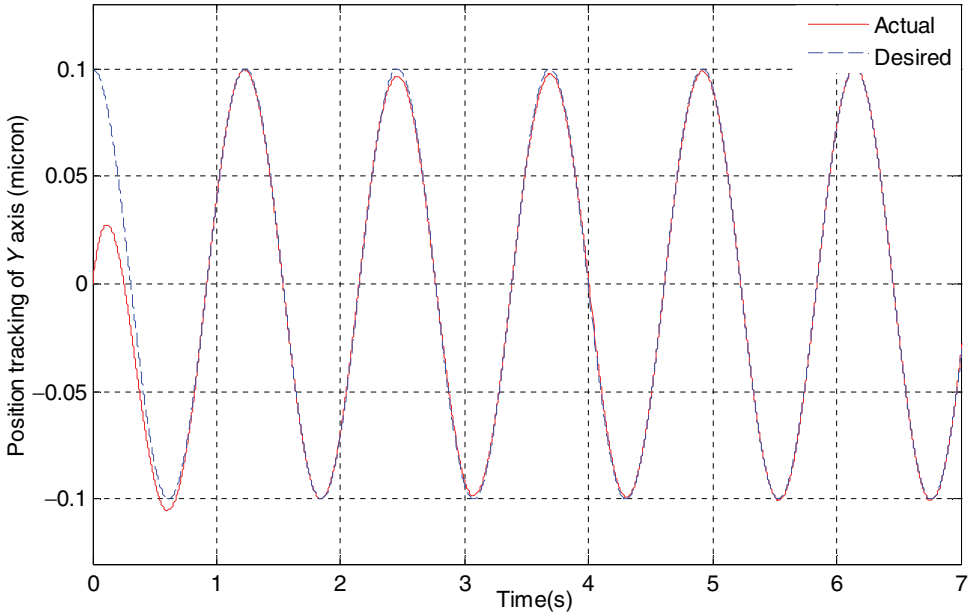

Fig. 12. Position tracking for y-axis under the RNSM controller.

Next, another RBF NN is adopted to replace the fixed estimate of the upper bound of the NN modeling error and external disturbances in the design of robust compensator. We also took 45 hidden nodes in the second RBF NN and the learning rate in the adaptive algorithm of $\hat{\boldsymbol{\theta}}$ is designed as $\eta = 5$. Figs. 9 and 10 show the tracking performance under the adaptive sliding mode compensator (ASMC).

Now, let the external disturbance multiply 100 times and it becomes $\boldsymbol{\tau}_d = 100[(\sin(6.17t))^2 + \cos(5.11t), (\sin(5.11t))^2 + \cos(6.17t)]^{\mathrm{T}}$. Under fixed RNSM control, the results of position tracking and control inputs are shown in Figs. 11–13; Under the adaptive sliding mode compensator, the results are depicted in Figs. 14–16.

https://doi.org/10.1017/S026357471400160X Published online by Cambridge University Press

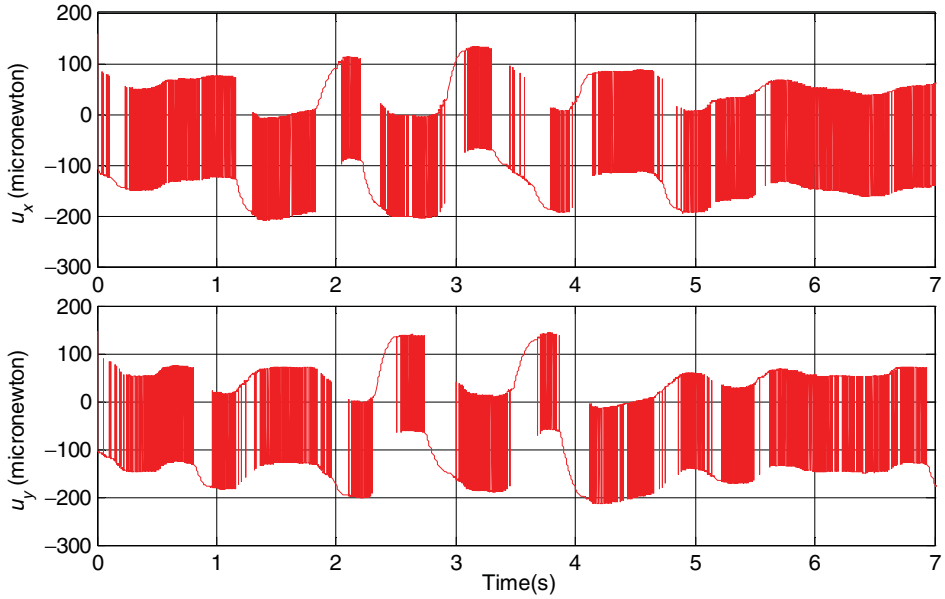

Fig. 13. Control inputs of the RNSM controller.

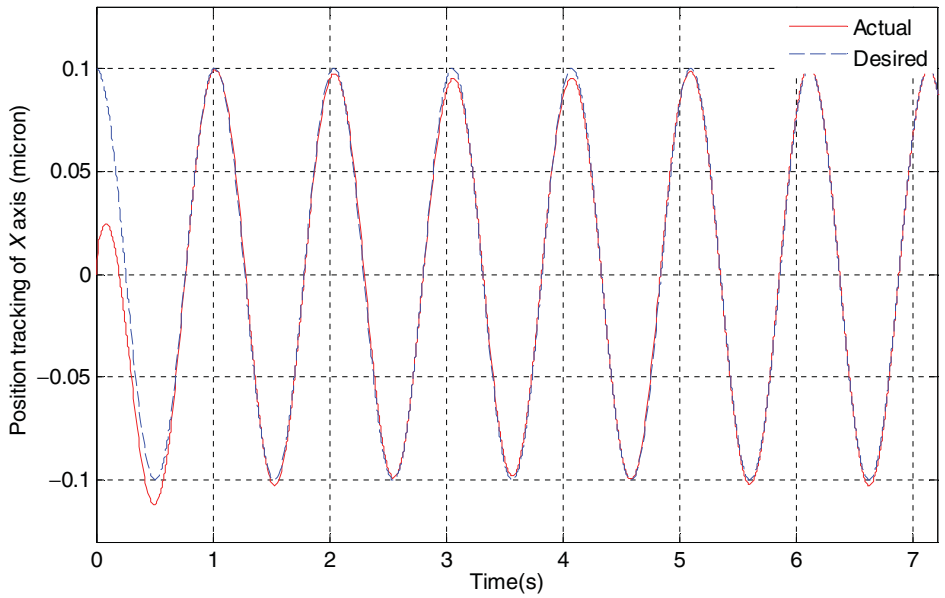

Fig. 14. Position tracking for the x-axis under ASMC.

As seen from the previous figures, although external disturbances become 100 times larger, the tracking error still converges to zero under both the fixed and the adjustable gain compensators, but their control inputs are remarkably different. Comparing Figs. 16 with 13, we can conclude that the adaptive sliding mode compensator can eliminate the chattering effectively.

https://doi.org/10.1017/S026357471400160X Published online by Cambridge University Press

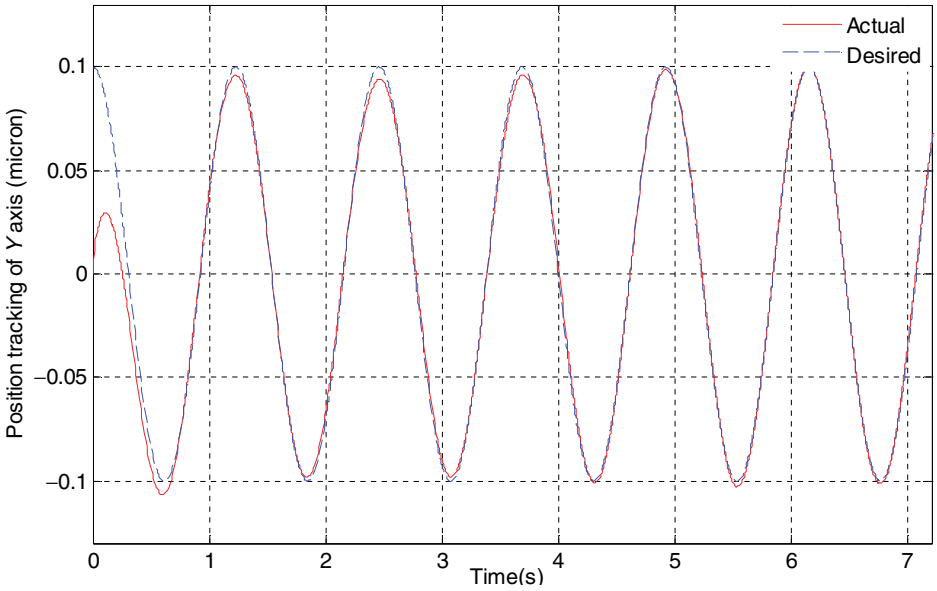

Fig. 15. Position tracking for *y*-axis under ASMC.

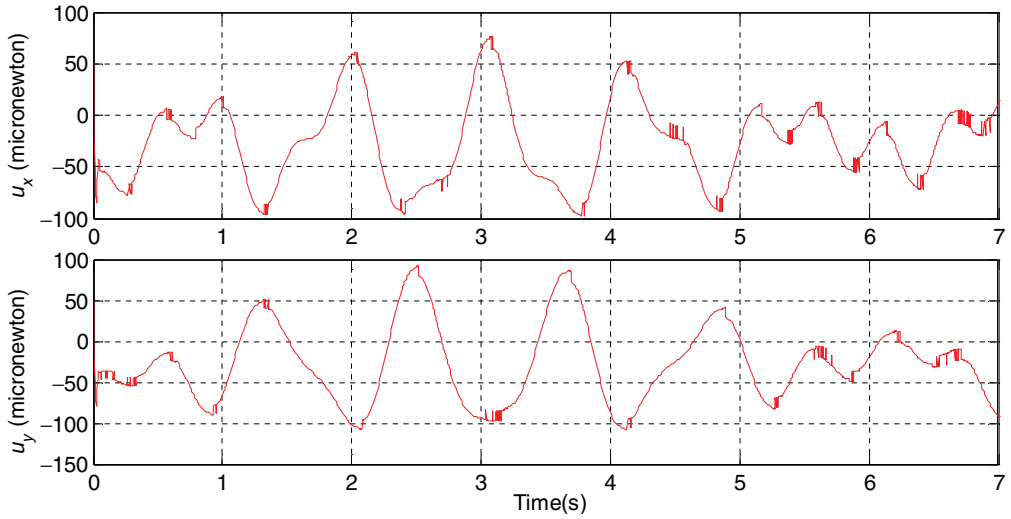

Fig. 16. Control inputs of ASMC.

6. Conclusion

A new robust neural sliding mode tracking control scheme using RBF NNs for vibratory angular velocity sensor has been developed in this paper. Several advantages of the proposed tracking control scheme have been summarized. These include a strong robustness property with respect to large system uncertainties and external disturbances, fast convergence of the tracking error to zero, and easy implementation for practical application. In the proposed control scheme, all the system dynamics can be unknown and the prior knowledge on the uncertain bound is not required. All adaptive learning algorithms were derived in the sense of Lyapunov stability analysis, so the stability of the closed-loop system can be guaranteed. A simulation example with a *z*-axis MEMS gyroscope is investigated to verify the effectiveness of the proposed control schemes.

Acknowledgements

The authors thank the anonymous reviewers for useful comments that have helped to improve the quality of the manuscript .This work is supported by the National Science Foundation of China

https://doi.org/10.1017/S026357471400160X Published online by Cambridge University Press

under Grant No. 61374100, the Natural Science Foundation of Jiangsu Province under Grant No. BK20131136, the University Graduate Research and Innovation Projects of Jiangsu Province under Grant No. CXLX12_0235, and the Fundamental Research Funds for the Central Universities under Grant Nos. 2013B24614, 2013B19314 and 2014B04014.

References

1. S. Park, "Adaptive control of a vibratory angle measuring gyroscope," *Sensors* **10**(9), 8478–8490 (2010).
2. R. P. Leland, "Adaptive control of a MEMS gyroscope using Lyapunov methods," *IEEE Trans. Control Syst. Technol.* **14**(2), 278–283 (2006).
3. M. Salah, M. McIntyre and D. Dawson, "Sensing of the time-varying angular rate for MEMS *Z*-axis gyroscopes," *Mechatronics* **20**(6), 720–727 (2010).
4. C. Wang and H. Yau, "Nonlinear dynamic analysis and sliding mode control for a gyroscope system," *Nonlinear Dyn.* **66**(1), 53–65 (2011).
5. J. Fei and Y. Yang, "Comparative study of system identification approaches for adaptive tracking of MEMS gyroscope," *Int. J. Robot. Autom.* **27**(3), 322–329 (2012).
6. B. Ebrahimi and M. Vali, "Terminal sliding mode control of *Z*-axis MEMS gyroscope with observer based rotation rate estimation," *Proceedings of the American Control Conference* (2011), pp. 3483–3489.
7. J. Fei, "Robust adaptive vibration tracking control for a MEMS vibratory gyroscope with bound estimation," *IET Control Theory Appl.* **4**(6), 1019–1026 (2010).
8. R. J. Wai, "Tracking control based on neural network strategy for robot manipulator," *Neurocomputing* **51**,425–445 (2003).
9. P. Patompark and I. Nilkhamhang, "Adaptive backstepping sliding-mode controller with bound estimation for underwater robotics vehicles," *Proceedings of the 9th International Conf. on Electronics, Computer, Telecommunications and Information Technology* (2012) pp. 1–4.
10. F. Lewis, A. Yesildirek and K. Liu, "Multilayer neural-net robot controller with guaranteed performance," *IEEE Trans. Neural Netw.* **7**(2), 388–399 (1996).
11. G. Feng, "A compensating scheme for robot tracking based on neural networks," *Robot. Auton. Syst.* **15**(3), 199–206 (1995).
12. F. Lin, S. Chen and K. Shyu, "Robust dynamic sliding-mode control using adaptive RENN for magnetic levitation system," *IEEE Trans. Neural Netw.* **20**(6), 938–951 (2009).
13. Z. Man, H. Wu, S. Liu and X. Yu, "A new adaptive backpropagation algorithm based on Lyapunov stability theory for neural networks," *IEEE Trans. Neural Netw.* **17**(6), 1580–1591 (2006).
14. J. Moody and C. J. Darken, "Fast learning in networks of locally-tuned processing units," *Neural Comput.* **1**(2), 281–298 (1989).
15. T. Holcomb and M. Morari, "Local training for radial basis function networks: Towards solving the hidden unit problem," *Proceedings of the American Control Conference* (1991) pp. 2331–2336.
16. J. Park and I. Sandberg, "Universal approximation using radial-basis-function networks," *Neural Comput.* **3**(2), 246–257 (1991).
17. F. Albertini and E. D. Sontag, "For neural nets, function determines form," *Proceedings of the 31st IEEE Conference on Decision and Control* (1992) pp. 26–31.
18. W. Grimm, "Robot non-linearity bounds evaluation techniques for robust control," *Int. J. Adapt. Control Signal Process*. **4**(6), 501–522 (1990).
19. K. Astrom and B. Wittenmark, *Adaptive Control* (Addison-Wesley, New York, 1995).
20. J. Slotine and W. Li, *Applied Nonlinear Control* (Prentice-Hall, Englewood Cliffs, NJ, 1991).
21. J. Fei, H. Ding, "Adaptive sliding mode control of dynamic system using RBF neural network," *Nonlinear Dyn*. **70**(2),1563–1573 (2012).
22. J. Fei and M. Xin, "An adaptive fuzzy sliding mode controller for MEMS triaxial gyroscope with angular velocity estimation," *Nonlinear Dyn* **70**(1), 97–109 (2012).
23. S. Park and R. Horowitz, "Adaptive control for the conventional mode of operation of MEMS gyroscope," *J. Microelectromech. Syst.* **12**(1), 101–108 (2003).
24. J. Fei and H. Ding, "System dynamics and adaptive control for MEMS gyroscope sensor," *Int. J. Adv. Robot. Syst.* **7**(4), 81–86 (2010).